Fuzzy C-means-driven FHCE contextual segmentation method for mammographic microcalcification detection

P Bougioukos[a], D Glotsos*[b], S Kostopoulos[a], A Daskalakis[a], I Kalatzis[b], N Dimitropoulos[c], G Nikiforidis[a] and D Cavouras[b]

[a]Medical Image Processing and Analysis Group, Laboratory of Medical Physics, Faculty of Medicine, University of Patras, Rio-Patras 26504, Greece

[b]Department of Medical Instruments Technology, Technological Educational Institute of Athens, Egaleo, Athens 12210, Greece

[c]EUROMEDICA, Department of Medical Imaging, Mesogeion Avenue, Athens 15125, Greece

Abstract: The frequency histogram of connected elements (FHCE) is a recently proposed algorithm that has successfully been applied in various medical image segmentation tasks. The FHCE is based on the idea that most pixels belong to the same class as their neighbouring pixels. However, the FHCE performance relies to a great extent on the optimal selection of a threshold parameter. Since evaluating segmentation results is a highly subjective process, a collection of threshold values must typically be examined. No algorithm has been proposed to automate the determination of the threshold parameter value of the FHCE. This study presents a method based on the fuzzy C-means clustering algorithm, designed to automatically generate optimal threshold values for the FHCE. This new approach was applied as a part of a structured sequence of image processing steps in order to facilitate segmentation of microcalcifications in digitized mammograms. A unique threshold value was generated for each mammogram, taking into account the different grey-level patterns based on different compositions of various breast tissues in it. The segmentation algorithm was tested on 100 mammograms (50 collected from the Mammographic Image Analysis Society and 50 normal mammograms onto which a number of simulated microcalcifications were generated). The algorithm was able to detect subtle microcalcifications with sensitivity ranging from 93 to 98%, False alarm ratio from 3 to 5% and false negatives variability from 2 to 3%.

Keywords: mammography, microcalcification, image enhancement, automatic thresholding, image segmentation

1 INTRODUCTION

Diagnostic mammography is currently the most reliable method for the early detection of breast cancer.[2] Among the most important signs indicating the presence of malignant lesions is the existence of masses, microcalcifications (mCs) and clusters of mCs. However, in early stage cancer, the subtle differences between normal and abnormal tissues have been proven challenging for viewing even by experienced physicians:[3] up to 30% of breast lesions are missed during routine diagnosis.[4] This is one of the reasons why mammograms are considered to be

The MS was accepted on publication on 27 October 2009.

* *Corresponding author: Dimitrios Glotsos, PhD, Medical Image and Signal Processing (medisp) Lab., Department of Medical Instruments Technology, Technological Educational Institute of Athens, Ag. Spyridonos Street, Egaleo 12210, Greece; email: dimglo@teiath.gr*

IMAG mp195 © RPS 2010 DOI: 10.1179/136821909X12581187860095

among the most difficult to interpret types of medical images. Another important reason is the low contrast appearance of early stage abnormalities (such as mCs) and their low differentiation from surrounding breast tissues.[5] mCs should appear as bright spots. However, in many cases, due to the composition of surrounding breast tissues and imaging limitations, mCs appear as low contrast entities.

Various screening programs[6] and research studies[7] have attempted to assess the importance of mCs in breast cancer. Although different reports have been documented, most of these studies and programmes seem to agree on the fact than mCs, which occur in both normal and abnormal breast tissues, constitute early stage indications of potential abnormalities. Among most recent studies, such as in Ref. 8, it is reported that the frequency of malignancy for women with high risk of breast cancer presenting mCs was 70%, which is significantly higher than other women.

The positive influence of computer-aided detection (CAD) of mCs on the improvement of diagnosis has been extensively investigated.[9–17] Research studies[18] have given different insights into the basic parts of a CAD system: the segmentation of suspicious for containing mCs regions of interest (ROIs) and the characterisation of these regions as normal, benign or malignant. These studies have mostly utilized publicly available digital material, such as the mammographic Image Analysis Society (MIAS)[19] and Digital Database for Screening Mammography databases.[20] Computational approaches include, among others, iterative threshold methods combined with fuzzy logic,[21] intensity-based local thresholding[22] and morphological filtering,[23,24] multi-fractal analysis, combined with mathematical morphology,[25] pattern recognition methods employing neural networks[1] and advanced contrast enhancement methods.[1] Although these studies present promising results, their application to daily clinical practice is very difficult, since extensive experimentation and definition of user-input parameters (i.e. threshold value, window size and number of iterations) are required for optimal segmentation of microcalcifications.

Another technological advance in the field of medical image segmentation is the recently introduced concept of the frequency histogram of connected elements (FHCE).[1] The FHCE algorithm is based on the idea that most pixels belong to the same class as their neighbouring pixels. Under this perspective, any object that consists of only 1 pixel has a very low probability of occurring under the FHCE assumption. This method has been tested on challenging medical image segmentation problems, such as in vessels segmentation on digital subtraction angiographies with promising results.[1] The FHCE algorithm exploits contextual information to extract the objects of interest resembling the decision making process of physicians, who assess the nature of mCs by examining their spatial neighbourhood. Thus, the FHCE could be a potential candidate solution to automated detection of mCs.

However, the FHCE performance relies to a great extent on the optimal selection of a threshold parameter. Since evaluating segmentation results is a highly subjective process, a collection of threshold values must typically be examined, since no algorithm has been proposed to specify and automate the determination of the threshold parameter value. The threshold parameter has been shown to vary significantly not only between images of different type but also between images within the same database (i.e. from mammogram to mammogram). Since mCs are considered as low contrast entities, a unique value for the threshold parameter suitable for any mammograms is very difficult, if not impossible, to define.

This study presents a method based on fuzzy C-means (FCM) clustering algorithm, designed to automatically generate optimal threshold values for the FHCE. This new approach was applied as a part of a structured sequence of image processing steps in order to facilitate segmentation of mCs in digitized mammograms. A unique threshold value was generated for each mammogram, taking into account the different compositions of various breast tissues in each mammogram. In this way, the algorithm is parameter-free, in the sense that the critical value of the threshold is automatically and independently estimated for each mammogram.

2 METHODS AND MATERIALS

The performance of the proposed algorithm in automated mCs detection was tested on two individual databases: The first database comprised 50 images (1024 × 1024 × 8 bit), collected from the MIAS database.[19] MIAS is considered as benchmark database widely used by researchers, with hundreds of citations. It contains mammograms extracted from the UK National Breast Screening programme. The database contains MLO views of both left and right breasts with pathologically confirmed abnormalities

of known coordinates (if any) and different density types (fatty, fatty-granular and dense-granular). Classifications have been made according to BIRADS standard. Since MIAS database has been extracted from the UK National Breast Screening programme, it can be argued that the dataset contain cases representative of standard cases a radiologist might face in clinical practice. The exact location (coordinates) of mCs was known on each mammogram. The second database comprised 50 mammograms with no abnormal findings, which were obtained by a General Electric DMR Plus mammographic unit with molybdenum/molybdenum (Mo/Mo) anode/filter combination and 650 mm focus to film distance and were digitized on a Microtec Scanmaker II SP (1200 × 1200 dpi, 8 bit grey-level). All mammograms were supplied by the Department of Medical Imaging, EUROMEDICA Medical Centre, Athens, Greece. On the digitized mammograms, a number of simulated mCs were modelled and generated at various anatomical locations (breast parenchyma, periphery, etc.), as it has been previously described.[26]

A radiologist (N. Dimitropoulos) examined the images, indicated the number of mCs (golden standard for the evaluation of our method) that existed on the images, and he marked the regions that contained the identified mCs. The marked regions were processed for the automated segmentation of mCs.

The implementation of the proposed segmentation algorithm was performed within a sequence of image processing steps comprising:

- high-pass filtering,[27] as a pre-filtering step for enhancing medium-to-high frequency information and boosting the performance of the contrast limited adaptive histogram equalisation (CLAHE),[28] which was designed and tuned for contrast enhancement of mCs
- background correction,[27] for suppressing structural noise, i.e. breast tissues other than mCs
- unsupervised classification,[27] for the automatic determination of the optimum threshold of the FHCE algorithm, which performed the final segmentation of the regions that contained mCs.

2.1 High-pass and CLAHE filtering

High-pass filters have been shown to be efficient as a pre-processing step in emphasizing objects with high intensity[29] (microcalcifications). In this step, several high-pass filters were tested for determining the filtering mask providing with best image quality. The latter was indicated by the experienced radiologist (N. Dimitropoulos) (Figs. 1c and 2c), who took under consideration various breast image parameters, such as specific anatomical structures and presence of noise or artefacts. The high-pass filtering mask that was utilized is depicted in Fig. 3. The frequency spectrum of the high-pass filter is shown in Fig. 4; white, grey and black correspond to high, medium and low spectral values respectively.

Following the high pass filtering, the CLAHE algorithm was applied. CLAHE maximizes the contrast throughout the image by adaptively enhancing the contrast of each pixel relative to its local neighbourhood.[1] According to CLAHE, the image is initially divided into a number of non-overlapping contextual regions of equal sizes. For every contextual region, its histogram is calculated. A clip limit for clipping histograms is then specified. The clip limit is a threshold parameter by which the contrast of the image can be effectively altered: a higher clip limit increases image contrast. The histogram of every contextual region is redistributed in such a way that its height does not exceed the clip limit. Finally, the neighbouring tiles are combined, using bilinear interpolation, and the image grey-levels are modified according to the cumulative distribution function of each tile.[27] As result of applying CLAHE on the image, mCs, which are bright spots, become brighter with respect to their neighbouring pixels, thus improving mCs' visualisation.

2.2 Background removal

In order to enhance the visibility and detectability of mCs, a structural noise (background-tissue) removal technique was implemented. Initially, a morphological opening[30] was applied, in order to create an image in which the grey-pixel values corresponded to the breast tissue. Thus, the background image was obtained. Subsequently, the generated background image was subtracted from the original mammographic image. The result of this procedure facilitated the segmentation procedure, since mCs appeared as bright white spots in a darker background.

2.3 Frequency histogram of connected elements technique

FHCE[1] relies on the concept of the morphological component or neighbourhood, which is similar to the

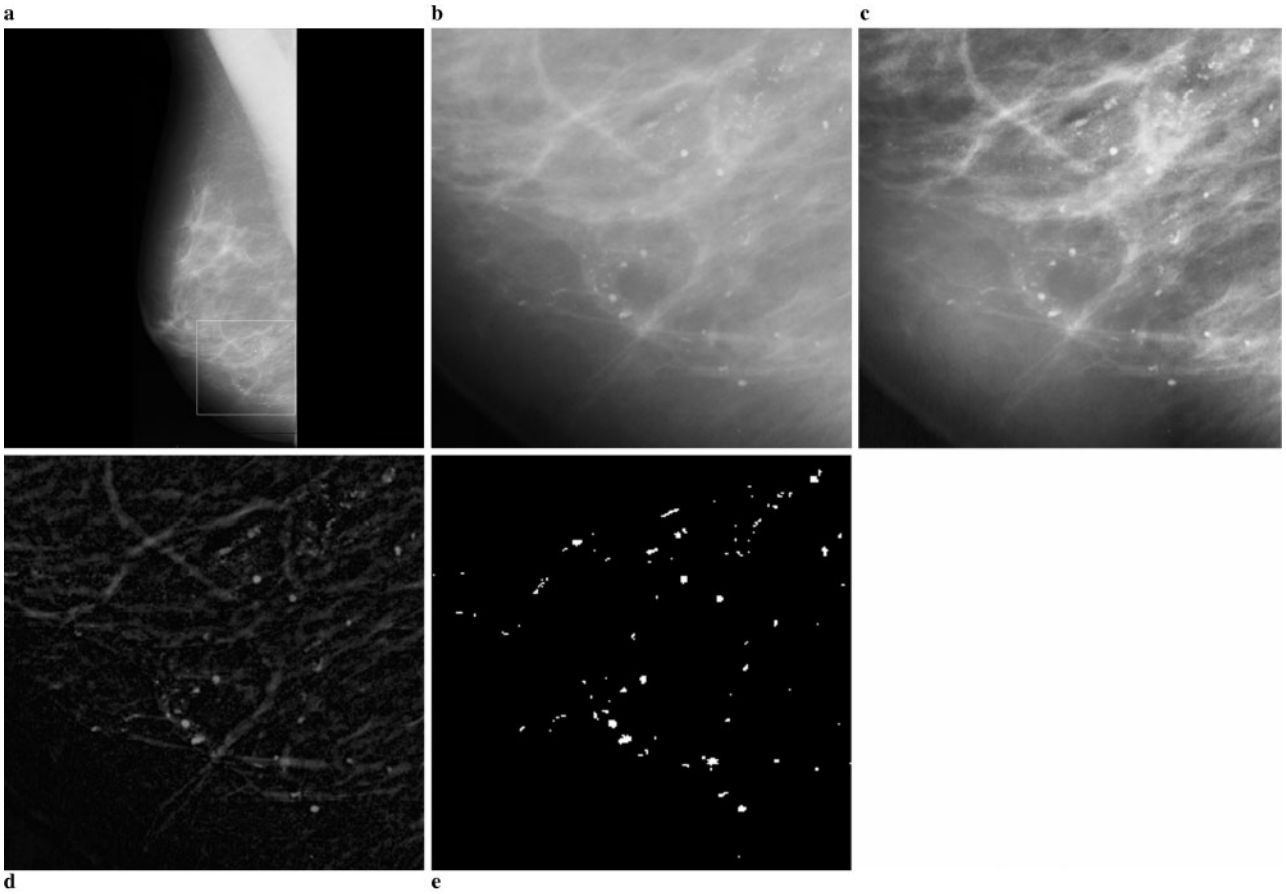

1 Steps of segmentation procedure using the proposed methodology: (a) original images containing (MCCs); (b) region of interest (ROI); (c) the enhanced ROI using the high-pass and CLAHE filters; (d) after background removal; (e) segmented image using the FHCE algorithm

methods used in morphological image processing. If $I(i,j)$ is a digital image with $N \times M$ dimensions, then for a given pixel (i,j), the neighbourhood of this pixel $D(i,j)$ is defined as

$$D(i,j) \triangleq \left\{\phi_{i,j} \subset \{I(i,j)\}_{\mathrm{N}\times\mathrm{M}}\right\} \quad (1)$$

where $\phi(i,j)$ is a user-defined window used in the scanning process. Scanning is performed by dividing the whole image into a set of non-overlapping windows. The window size relies on the selection of the morphological component. Non-overlapping windows were selected to reduce computational burden.

The morphological component is a very crucial parameter in order to obtain the final desired output (the segmented image). The morphological component is a mask, which determines the shape of the connected element (described below). For example, if the Mask 1 is applied, the connected element is a line vector mask. In this paper, five different masks[30] were tested as morphological components (Fig. 5). Owing to the small size of masks (3×3) and large size of images (1024×1024 and 1200×1200), border pixels (one pixel wide) were considered as of limited importance and were left untreated.

Based on the morphological component, the connected element was defined, which is another parameter used in the FHCE approach. The connected element is any neighbourhood unit, such that its pixels belong to the range $[T-c, T+c]$, where c is an integer defining the greyscale intensity range of the neighbourhood and T is a given greyscale value.[1] Parameter c is calculated as the ratio of maximum to minimum value occurring at every position of the scanning window (morphological component). Thus, there is no global value for c for each mammogram; the value of c varies depending on neighbourhood values at every scanning window. The number of connected elements constitutes the FHCE histogram.

In the ideal situation, optimum results could be obtained if the distributions of the pixels in the

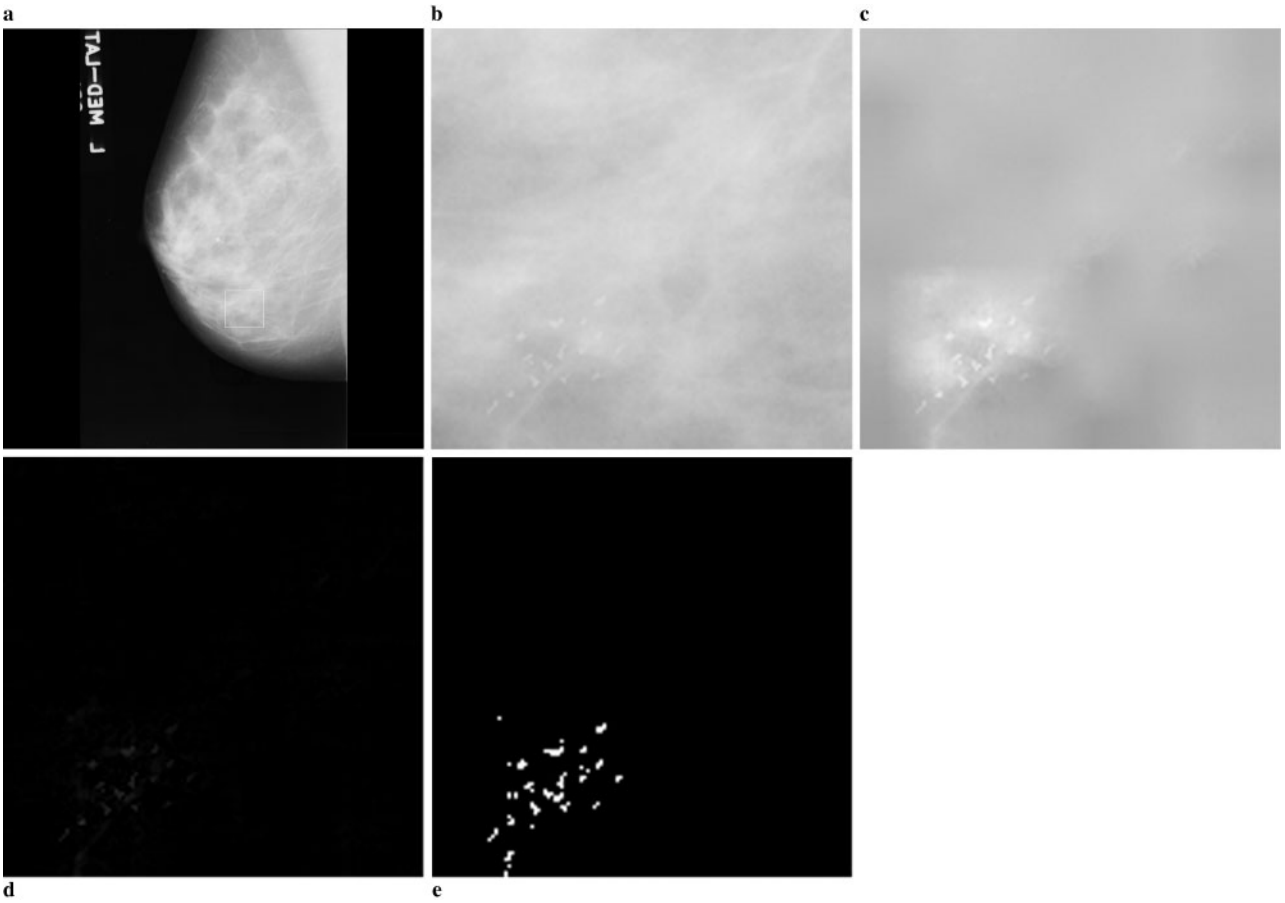

2 Mammogram containing simulated microcalcifications: (a) original images containing simulated mCs; (b) region of interest (ROI); (c) the enhanced ROI using the high-pass and CLAHE filters; (d) after background removal; (e) segmented image using the FHCE algorithm

FHCE histogram were well apart, constituting two peaks corresponding to background and mCs. Then, the final segmentation could be obtained by setting a threshold value between those two peaks.

The threshold of the FHCE algorithm was calculated using an FCM algorithm that was designed to seek for two data clusters of connected elements: the first cluster that corresponded to connected elements belonging to mCs and the second cluster related to the surrounding background class. According to the aforementioned procedure, the optimum threshold parameter resulted as the intersection of the median of the two cluster centroids with the greyscale axis.

$$High-Pass=\begin{pmatrix}1 & -4 & 1\\ -4 & 16 & -4\\ 1 & -4 & 1\end{pmatrix}$$

3 Appropriate high-pass filter proved to be efficient as a pre-processing step in emphasizing objects with high intensity

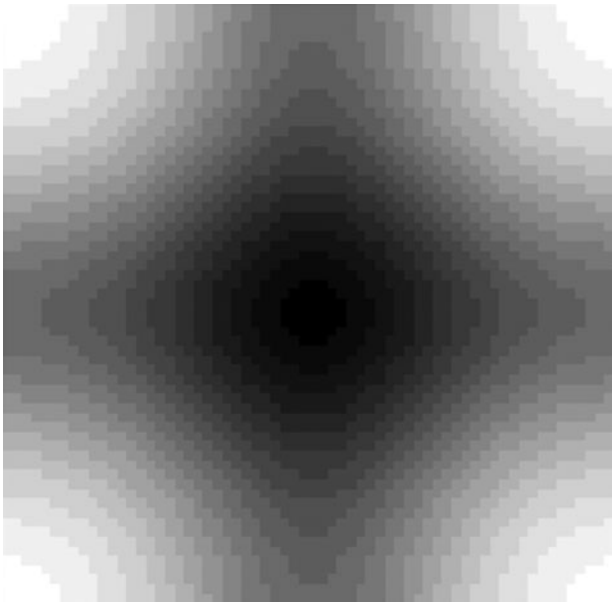

4 Frequency spectrum of the utilized high-pass filter. White, grey and black corresponds to high, medium, and low spectral values respectively

$Mask1=\begin{pmatrix}0&0&0\\1&1&1\\0&0&0\end{pmatrix}$	$Mask2=\begin{pmatrix}0&1&0\\0&1&0\\0&1&0\end{pmatrix}$	$Mask3=\begin{pmatrix}0&1&0\\1&1&1\\0&1&0\end{pmatrix}$
$Mask4=\begin{pmatrix}1&0&1\\0&1&0\\1&0&1\end{pmatrix}$	$Mask5=\begin{pmatrix}1&1&1\\1&1&1\\1&1&1\end{pmatrix}$	

5 Various masks tested to be used as morphological components

The FCM is an iterative clustering algorithm, which finds cluster centres (centroids) that minimize the dissimilarity function

$$J(U, c_1, c_2, \cdots, c_c) = \sum_{i=1}^{c} J_i = \sum_{i=1}^{c}\sum_{j=1}^{n} u_{ij}^{m} d_{ij}^{2} \qquad (2)$$

where c_i is the centroid of cluster i, $d_{i,j}$ is the Euclidian distance between the ith centroid (c_i) and jth data point, $u_{i,j}$ is the element of a fuzzy membership function matrix $U=u_{i,j}$ with values $0 \leqslant u_{i,j} \leqslant 1$, and m is a weighting exponent (the value of m was experimentally determined for optimum results as $m=2$).

During iteration, the algorithm modifies the cluster centres and changes the data memberships until the dissimilarity function is minimized.

2.4 Evaluation

To evaluate the results, the segmented binary objects correctly identified as mCs by the present method were considered as true positives (TP). False positives (FP), false negatives (FN) and true negatives (TN) cases represented the erroneously segmented or missed mCs respectively. Additionally, the terms of sensitivity and the false alarm ratio (FAR) were evaluated

$$\text{Sensitivity} = \frac{\text{TP}}{\text{TP}+\text{FN}}$$
$$\text{FAR} = \frac{\text{FP}}{\text{FP}+\text{TN}} \qquad (3)$$

3 RESULTS

The algorithm was able to detect subtle mCs and its results were most promising. In Table 1, the evaluation results of the proposed segmentation method are demonstrated. Sensitivity ranged between 93 and 98%. The FAR was 3–5% and FN variability was 2–3%.

The morphological component is a very significant parameter in the resulting image. The best result (Fig. 6d–f) was gained utilizing Mask 1, Mask 2 and Mask 3 in the ROI pre-defined by the radiologist, which contained mMs.

The required steps for obtaining the resulting segmented image are depicted below. In the original image, a ROI was specified (Figs. 1a and 2a). In this ROI (Figs. 1b and 2b), the pre-processing step was accomplished by applying the high-pass and the CLAHE filters (Figs. 1c and 2c). Figures 1d and 2d demonstrate image background removal. Eventually, the resulting image was introduced to the modified FHCE algorithm, in order to obtain the segmented one (Figs. 1e and 2e).

4 DISCUSSION

FHCE has already been proven powerful in medical image segmentation tasks.[1] However, it presents a major challenge, that is, the determination of a threshold parameter suitable for dividing the histogram of connected elements into different biologically meaningful regions. The threshold value is user-dependent. After extensive experimentation with various user-defined thresholds for the task of mCs segmentation in digitized mammograms, two important observations were made:

1. FHCE gave promising results in mCs segmentation, but there was no global threshold value applicable for all mammograms; threshold values changed significantly from mammogram to mammogram, especially for breasts with different parenchyma compositions.
2. The values of connected elements that the FHCE computed were found to tend to cluster into two major groups: one group corresponding to connected elements of mCs and another group corresponding to connected elements of surrounding breast, independently of the composition of the breast parenchyma.

Table 1 Microcalcification detection performance in 100 mammograms

Evaluation parameters	Range (%)
Sensitivity	93–98
True positives (TP)	93–98
False positives (FP)	3–5
False alarm ratio (FAR)	3–5
False negatives (FN)	2–3

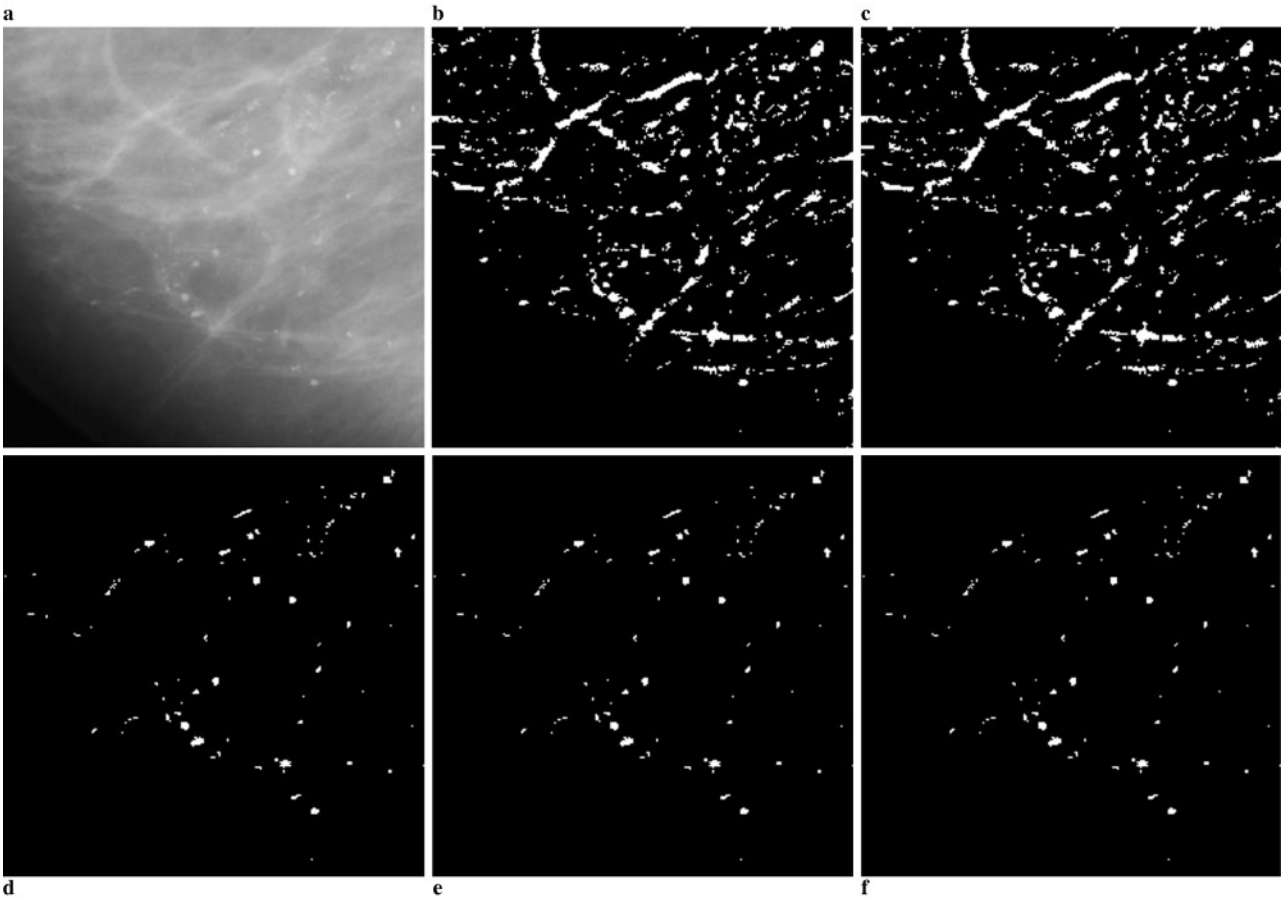

6 ROI containing microcalcifications (a) segmented using the five different morphological components (b–f)

The latter observation was integrated within the FHCE by incorporating an unsupervised FCM classifier that converged automatically to a certain threshold value for each image. This value was assumed to be the intersection of the median between the two clusters centroids with the greyscale axis.

It has to be stressed that manual threshold selection by the experienced radiologist resulted in inferior sensitivity (85–91%) in mC detection than the proposed automatic approach (93–98%); since comparison was based on ground-truth data (MIAS and simulated with mC images), it is argued the FCM driven selection process results in an optimal threshold taking into account the individuality of each mammogram (regarding both composition of different breasts and specification of imaging system acquiring mammograms).

Apart from the threshold value, another important setting for the FHCE algorithm is the morphological component selection. Five different morphological components were tested. Experimental results highlighted the 'cross-shaped' mask (Mask 3), the 'x-shaped' mask (Mask 4) and the 'box-shaped' mask (Mask 5) as the most efficient. The 'horizontal' (Mask 1) and 'vertical line-shaped' (Mask 2) components did not work satisfactory. These components encode properties of horizontal and vertical directionality, mixing mCs with vessels spreading across the horizontal or vertical direction (Fig. 6b and c). On the other hand, the 3 pixel sized masks (cross, x and box) successfully eliminated vessels and surrounding breast tissue, while preserving mCs, which are small-sized compact-shaped structures with no directional preference (Fig. 6d–f).

Since mCs are tiny deposits of calcium within the breast, one would expect that their detection would be relatively straightforward. mCs should appear in the mammographic image as bright objects due to the existence of calcium. However, very frequently mCs are missed in most mammograms, especially when their location lies within dense breast tissues.[20,31–33] The simulated mCs images proved to be helpful to the evaluation of the proposed method for various types

of breast parenchyma and especially in dense breast tissues. The simulation model[20,32,34] allowed for the creation of mCs of various intensities, sizes, shapes and number of mCs per cluster. By computing the mean grey level of pixels belonging to the background (surrounding tissue), mCs were generated with pixels intensities ranging from five to 20 times higher compared to background. mCs generated with lower pixel intensities simulated early stage abnormalities located into dense breast tissues. In this way, it was possible to quantitatively assess the pixel intensity that a mCs should exhibit with respect to surrounding background, in order to be detectable by the proposed algorithm. This minimum fraction was defined as 6/1, meaning that mCs with six times higher pixel intensity compared to the surrounding breast tissue were detectable. The mCs that were simulated differed from the background in a range from 2 to 10 grey-pixel values. The overall sensitivity of the proposed segmentation procedure ranged from 93 to 98% with two to three FN. FN mostly occurred in areas of low optical density. These results are in line with those reported in the literature[9–17] ranging from 92 to 95.8%; however, it has to be stressed that our method merits, compared to the above studies, in three major issues:

1. It is parameter-free in the sense that the critical value of the threshold parameter, which most studies eventually use at some point, is automatically estimated.
2. It is independent of the position of mCs within the breast anatomy.
3. It uses the concept of contextual segmentation that resembles the diagnostic procedure, followed by physicians during visual detection of mCs.

Thus, the proposed segmentation scheme has great potential to be used in conjunction to visual inspection for the detection of mMs in routine diagnosis.

REFERENCES

1 Patricio, M. A. and Maravall, D. A comparative study of contextual segmentation methods for digital angiogram analysis. *Cybern. Syst*., 2004, **35**, 63–83.

2 Sabel, M. and Aichinger, H. Recent developments in breast imaging. *Phys. Med. Biol*., 1996, **41**, 315–368.

3 Bazzocchi, M., Facecchia, I., Zuiani, C., Londero, V., Smania, S., Bottigli, U. and Delogu, P. Application of a computer-aided detection (CAD) system to digitalized mammograms for identifying microcalcifications. *Radiol. Med*., 2001, **101**, 334–340.

4 Cheng, H. D., Cai, X., Chen, X., Hu, L. and Lou, X. Computer-aided detection and classification of microcalcifications in mammograms: a survey. *Patt. Recogn*., 2003, **36**, 2967–2991.

5 Nakayama, R., Abe, H., Shiraishi, J. and Doi, K. Potential usefulness of similar images in the differential diagnosis of clustered microcalcifications on mammograms. *Radiology*, 2009, **253**, 625–631.

6 Stewart, J. A. Breast cancer: 1. Screening and early management. *Hosp. Pract*., 1994, **29**, 81–85, 89–90.

7 Takako, M., Maya, Y., Akiko, K., Sumiya, N., Chika, H. and Tokiko, E. A comparison between film-screen mammography and full-field digital mammography utilizing phase contrast technology in breast cancer screening programs. *Lect. Notes Comput. Sci*., 2008, **5116**, 48–54.

8 Uematsu, T., Kasami, M. and Yuen, S. A cluster of microcalcifications: women with high risk for breast cancer versus other women. *Breast Cancer*, 2009, **16**, 307–314.

9 Mavroforakis, M., Georgiou, H., Dimitropoulos, N., Cavouras, D. and Theodoridis, S. Significance analysis of qualitative mammographic features, using linear classifiers, neural networks and support vector machines. *Eur. J. Radiol*., 2005, **54**, 80–89.

10 Papadopoulos, A., Fotiadis, D. and Likas, A. Characterization of clustered microcalcifications in digitized mammograms using neural networks and support vector machines. *Artif. Intell. Med*., 2005, **34**, 141–150.

11 Karssemeijer, N., Otten, J. D. M., Rijken, H. and Holland, R. Computer aided detection of masses in mammograms as decision support. *Br. J. Radiol*., 2006, **79**, S123–S126.

12 Karssemeijer, N., Otten, J. D., Verbeek, A. L., Groenewoud, J. H., de Koning, H. J., Hendriks, J. H. and Holland, R. Computer-aided detection versus independent double reading of masses on mammograms. *Radiology*, 2003, **227**, 192–200.

13 Rangayyan, R. M., Mudigonda, N. R. and Desautels, J. E. Boundary modelling and shape analysis methods for classification of mammographic masses. *Med. Biol. Eng. Comput*., 2000, **38**, 487–496.

14 Nandi, R. J., Nandi, A. K., Rangayyan, R. M. and Scutt, D. Classification of breast masses in mammograms using genetic programming and feature selection. *Med. Biolog. Eng. Comput*., 2006, **44**, 683–694.

15 Ferrari, R. J., Rangayyan, R. M., Desautels, J. E., Borges, R. A. and Frère, A. F. Identification of the breast boundary in mammograms using active contour models. *Med. Biolog. Eng. Comput*., 2004, **42**, 201–208.

16 Mu, T., Nandi, A. K. and Rangayyan, R. M. Classification of breast masses using selected shape, edge-sharpness, and texture features with linear and kernel-based classifiers. *J. Digital Imag*., 2008, **21**, 153–169.

17 Suliga, M., Deklerck, R. and Nyssen, E. Markov random field-based clustering applied to the segmentation of masses in digital mammograms. *Comput. Med. Imag. Graph*., 2008, **32**, 502–512.

18 Heath, M., Bowyer, K., Kopans, D., Moore, R. and Kegelmeyer, P. The digital database for screening mammography, Proc. 3rd Int. Workshop on Digital mammography, June 1996, Chicago, IL, USA, Medical Physics Publishing, pp. 212–218.

19 Suckling, J. The Mammographic Image Analysis Society digital mammogram database, Proc. 2nd Int. Workshop on Digital Mammography, York, UK, July 1994, York, Elsevier, pp. 375–378.

20 Davies, D. H. and Dance, D. R. Automatic computer detection of clustered calcifications in digital mammograms. *Phys. Med. Biol*., 1990, **35**, 1111–1118.

21 Fu, J. C., Leeb, S. K., Wongc, S. T. C., Yeha, J. Y., Wanga, A. H. and Wud, H. K. Image segmentation feature selection and pattern classification for mammographic microcalcifications. *Comput. Med. Imag. Graph*., 2005, **29**, 419–429.

22 Abdul-Karim, M. A., Al-Kofahi, K., Brown, E. B., Jain, R. K. and Roysam, B. Automated tracing and change analysis of angiogenic vasculature from *in vivo* multiphoton confocal image time series. *Microvasc Res*, 2003, **66**, 113–125.

23 Panchal, R. and Verma, B. Neural-association of microcalcification patterns for their reliable classification in digital mammography. *Int. J. Patt. Recogn. Artif. Intell*., 2006, **20**, 971–983.

24 Chitre, Y., Dhawan, A. T. and Moskowitz, M. Artificial neural network based classification of mammographic microcalcifications using image structure features. *Int. J. Patt. Recogn. Artif. Intell*., 1993, **7**, 1377–1401.

25 Stoutjesdijk, M. J., Veltman, J., Huisman, H., Karssemeijer, N., Barentsz, J. O., Blickman, J. G. and Boetes, C. Automated analysis of contrast enhancement in breast MRI lesions using mean shift clustering for ROI selection. *J. Magn. Reson. Imag*., 2007, **26**, 606–614.

26 Theodoridis, S. and Koutroubas, K. Pattern Recognition, 1999 (Academic Press, New York).

27 Gonzalez, R. C. and Woods, R. E. Digital Image Processing, 1992 (Addison-Wesley, Reading, MA).

28 Pizer S. M. and Amburn, E. P. Adaptive histogram equalization and its variations. *Comput. Vision Graph. Image Process*., 1987, **39**, 355–368.

29 Xu, Y. and Pitot, H. C. A software package to improve image quality and isolation of objects of interest for quantitative stereology studies of rat hepatocarcinogenesis. *Comput. Methods Programs Biomed*., 2006, **81**, 236–245.

30 Soille, P. Morphological Image Analysis, 1999 (Springer, Berlin).

31 Ibrahim, N., Fujita, H., Hara, T. and Endo, T. Automated detection of clustered microcalcifications on mammograms: CAD system application to MIAS database. *Phys. Med. Biol*., 1997, **42**, 2577–2589.

32 Cheng, H. D., Lui, Y. M. and Freimanis, R. I. A novel approach to microcalcification detection using fuzzy logic technique. *IEEE Trans. Med. Imag*., 1998, **17**, 442–450.

33 Papadopoulos, A., Fotiadis, D. I. and Likas, A. An automatic microcalcification detection system based on a hybrid neural network classifier. *Artif. Intell. Med*., 2002, **25**, 149–167.

34 Chan, H. P., Doi, K., Vyborny, C. J., Schmidt, R. A., Metz, C. E., Lam, K. L., Ogura, T., Wu, Y. Z. and MacMahon, H. Improvements in radiologists' detection of clustered microcalcifications on mammograms. The potential of computer-aided diagnosis. *Invest. Radiol*., 1990, **25**, 102–110.